Verification, Validation, and Limits of Applicability of a Rapid Bonded Joint Analysis Tool

Stephen P. Jones[1] and Bertram Stier[2]
Collier Research Corporation, Newport News, VA, 23606

Brett A. Bednarcyk[3] and Evan J. Pineda[4]
NASA Glenn Research Center, Cleveland, OH, 44135

Upul R. Palliyaguru[5]
National Institute for Aviation Research, Wichita, KS, 67260

Verification of stress analysis tools is a complex problem due to large numbers of input variables, wide ranges of typical values for each input, and lack of automation. Furthermore, it is often impossible to establish bounds within which a method produces accurate results due to the lack of sufficient benchmark data. In this paper, a verification process was implemented for a bonded joint analysis tool to compare virtual crack closure technique strength predictions with finite element analysis, as well as to approximate the limits of applicability of the tool with respect to material and geometric inputs. Excellent agreement was found, with the tool exhibiting a median difference of 5.2% compared to finite element analysis. The tool was further validated against test results, showing good agreement with typical error between 1% and 30%. Finally, the tool was implemented into the HyperSizer stress framework and is used for analysis and sizing of bonded joints using the same global load finite element models that engineers use for panel sizing.

I. Introduction

Stress analysis tools are often compared to benchmark results from literature as a form of verification [1] [2]. While this procedure may generate some confidence that the methodology has been implemented correctly, it is often not intended to provide an understanding of the overall accuracy of the tool. Additionally, the limits beyond which the new tool produces erroneous or unrealistic results (if they exist at all) are often not determined. While method developers may intuitively know the reasonable limits beyond which the results should not be trusted, typical stress engineers and end users do not share this understanding.

Validation to test data in many ways contrasts directly with verification. While verification is inexpensive (in terms of cost and time), validation is expensive. Verification often focuses on the adequacy of an implementation, whereas validation assesses an analysis tool against real-world results. Especially in the realm of rapid tools, where simplifications are expected to create some divergence from test results, there is a need to conduct an intermediate verification exercise. This exercise should confirm that a tool is producing results consistent with a similar (but not identical) approach to the problem, without introducing additional complexities inherent in more complex validation. Discrepancies with test data may arise from a huge array of sources, such as natural scatter, measurement uncertainty,

[1] Aerospace Structural Engineer, AIAA Member
[2] Research Engineer, Advanced Composites, AIAA Member
[3] Materials Research Engineer, AIAA Associate Fellow
[4] Aerospace Research Engineer, AIAA Senior Member
[5] Senior Research Engineer, Non-AIAA Member

manufacturing or material irregularities, or finite width (edge) effects. In order to decouple these effects from systematic inaccuracies inherent to the methodology, this intermediate verification is necessary.

In this work, the verification of the HyperSizer bonded joint analysis capability to FEA is described. The approach used to select, create, execute, and post-process thousands of unique analyses is documented. Additionally, limits of applicability are determined for the tool in order to advise users when the configuration being analyzed may not produce reliable results. A test plan was devised to validate the tool's virtual crack closure technique (VCCT) analysis methodology by testing a range of configurations of varying complexity. Specimens were manufactured and tested by the National Institute for Aviation Research (NIAR) in Wichita, Kansas. Finally, the rapid analysis tool was integrated into the latest version of the HyperSizer stress framework software.

II. Description of Bonded Joint Analysis Tool

A. Methodology

The HyperSizer bonded joint analysis tool is fundamentally based on Mortensen's unified approach [3], but has been significantly extended and has been implemented within the HyperSizer stress framework software since 2005 [4]. The methodology is formulated using plate theory kinematics, classical lamination theory (CLT), traction-separation equations in the adhesive, assumed cylindrical bending displacement fields in the adherends, and direct application of equilibrium between zones (see Fig. 1). Adhesive material behavior may be treated as linear or nonlinear, using the Ramberg-Osgood formulation [5] for the latter.

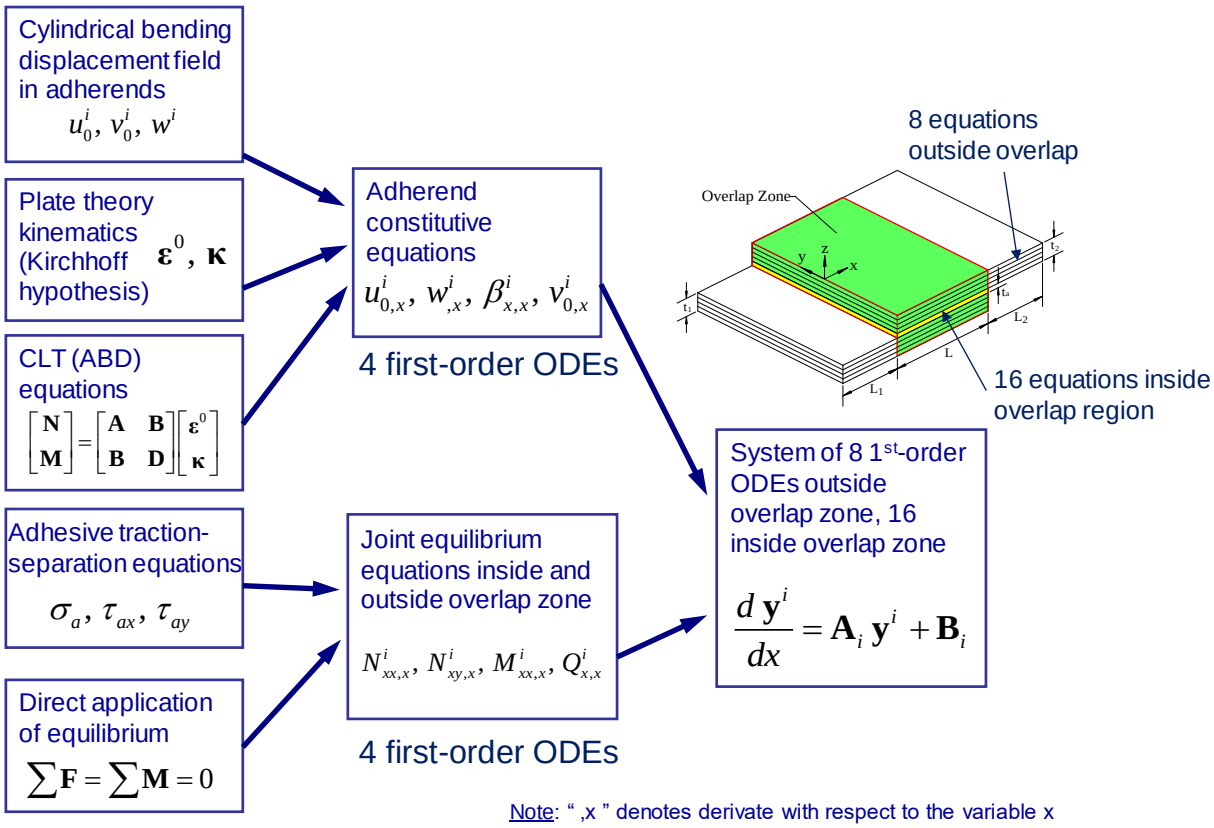

Fig. 1 Formulation of the system of ordinary differential equations (ODEs) in the analysis methodology

The system of ODEs is solved numerically, yielding laminate-level fields and adhesive stresses along the entire length of the joint. In-plane ply stresses and strains are calculated using Classical Lamination Theory (CLT). Out-of-plane (interlaminar) stress components are computed via through-thickness integration of the equilibrium equations. The full process of determining ply-by-ply three-dimensional stresses and strains has been previously documented in full [4].

The simplifying assumptions inherent in this methodology result in a highly efficient tool; typical execution time is in the range of a tens to hundreds of milliseconds. This speed enables the tool to be used for both analysis and sizing

when there may be tens of thousands of load cases and hundreds or thousands of unique joints in a large aerospace model.

B. Virtual Crack Closure Technique

In addition to assessing the strength of bonded joints using stress- or strain-based failure criteria [1], the virtual crack closure technique (VCCT) was implemented in the HyperSizer bonded joint analysis tool in 2006 [6]. VCCT has been used to supplement or replace stress-based failure criteria in composite bonded joints in the aerospace industry [7] [8] for a variety of reasons, including:

- VCCT is less sensitive to small model changes (or mesh density in the case of FEA) than stress-based criteria, because it is based on energy rather than stress
- Certification often requires that original equipment manufacturers (OEMs) account for potential defects in bondlines due to manufacturing flaws or in-service damage
- Required material properties are usually well-characterized through standard testing (critical strain energy release rates)

Although the HyperSizer bonded joint VCCT analysis capability is semi-analytical as opposed to the typical FEA-based implementations, it follows the same basic assumptions and process as its finite element equivalent. The HyperSizer-specific implementation has been previously described in published literature [6], and may be summarized according to conventional literature on the topic [9]. A pre-existing crack is included in the bondline of the model, and the work required to close the crack by an incremental Δa is used to compute the strain energy release rate according to equations 1 and 2, below.

$$G_I = -\frac{Z_i(w_l - w_{l*})}{2\Delta a} \tag{1}$$

$$G_{II} = -\frac{X_i(u_l - u_{l*})}{2\Delta a} \tag{2}$$

Where Z_i and X_i are the nodal force components at the crack tip, and w_l, w_{l*}, u_l and u_{l*} are the nodal displacements shown at nodes l and l*. This is shown graphically in Fig. 2 below.

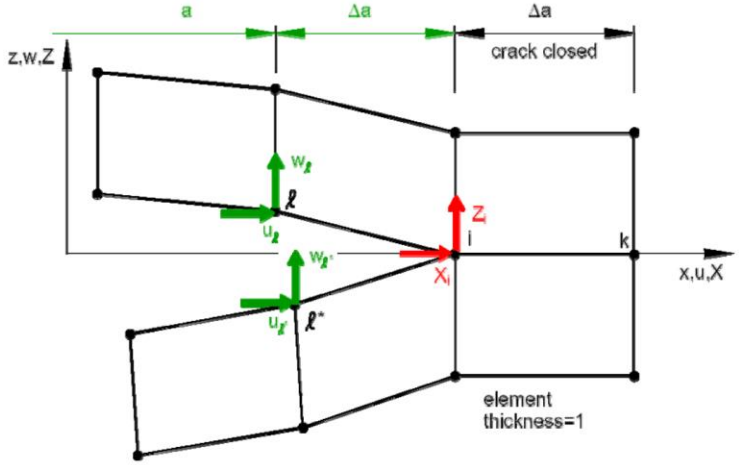

Fig. 2 Implementation of VCCT Within the Finite Element Method [9]

Following computation of the strain energy release rates, margins of safety are computed in HyperSizer by comparing these values against the critical strain energy release rates for the material. Several failure criteria are available, including interactive criteria such as power law and B-K [10].

C. Supported Joint Configurations

The HyperSizer bonded joint analysis capability supports a variety of joint configurations, as shown in Fig. 3 below. Within a given configuration (e.g. double strap), the joint geometry (such as overlap length or adhesive thickness) and material properties (such as adherend laminates) may be modified either by the user or as part of the sizing process.

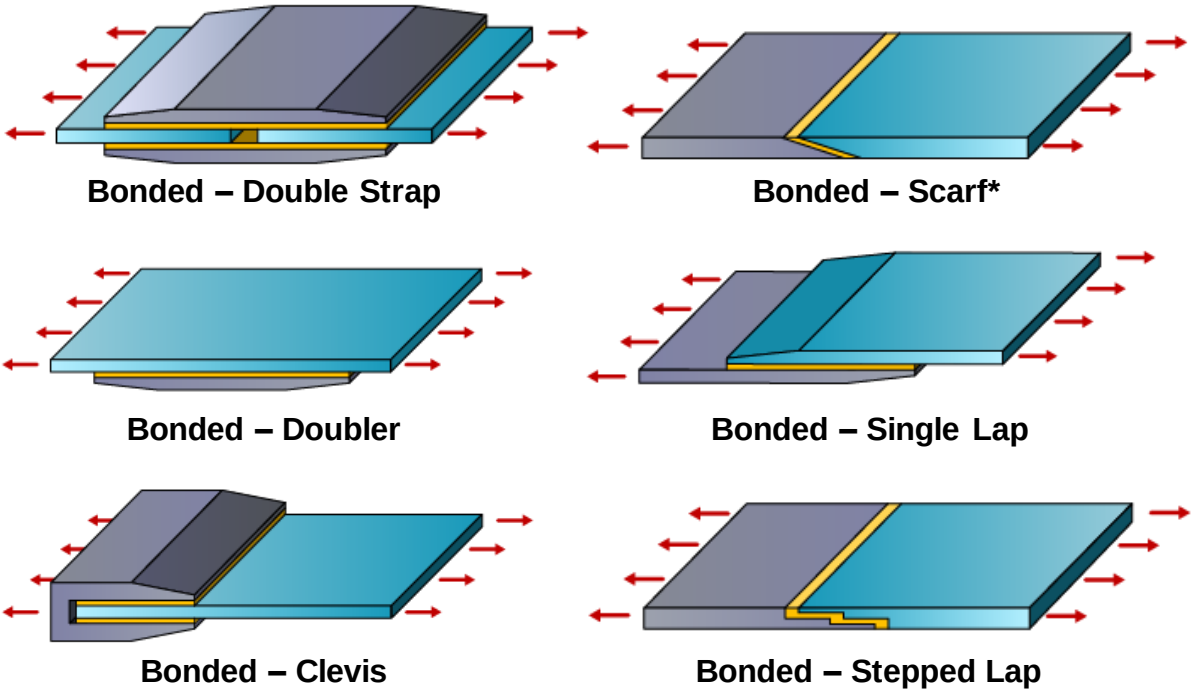

Fig. 3 HyperSizer Supported Bonded Joint Types (Scarf Joints Currently in Development)***

III. FEA Verification

As part of this collaborative research team member's effort under the NASA Advanced Composites Consortium (ACC), the HyperSizer bonded joint analysis tool was rigorously verified against FEA to confirm its accuracy in predicting crack growth. The objectives and processes implemented to complete this verification are described in this section.

A. Scope and Approach

As the HyperSizer bonded joint analysis capability had been previously verified and validated for its stress-based criteria [1] [4], the ACC verification effort focused on the growth of bondline cracks using VCCT. Of the joint configurations shown in Fig. 3, the following types were verified: single lap, doubler, step lap. The double strap and clevis joint had been previously verified [11], and the future verification of the scarf joint will be completed. Due to the desire to cover an extremely large design space for each joint configuration, efforts had to be undertaken to reduce the number of candidates to make computational execution feasible. The following approach was used.

1. Identify the bounds of each joint parameter (such as laminate thickness, overlap length, etc.) to encompass the design space of interest

This process is subjective, but based on engineering judgement of the typical applications of bonded joints. These bounds were selected to be broader than would typically be expected in actual joint configurations. Examples of bounds include:

- Adhesive modulus between 50ksi and 750ksi
- Adhesive thickness between 0.0001 inches and 0.2 inches
- Adherend ply counts between 2 and 200

2. Pseudo-randomly generate candidate designs for joints within this design space

During this step, all joint parameters (geometry, materials, and layups) are generated using the inbuilt Python random library. Some restrictions were implemented to prevent geometrically impossible configurations such as cases

where the initial crack length would be longer than the entire bondline. During this step applied loading is also determined. Because geometrically linear FEA was used, the **relative ratio** of axial force, bending moment, and transverse shear force were determined. In order to ensure sufficient diversity of laminate configurations, adherend laminates were selected from a pool of three categories:

- Purely randomly selected ply orientations and ply counts
- Balanced (but unsymmetrical) laminates
- Balanced and symmetric laminates

Although the bonded joint analysis tool is general enough to analyze laminates that contain arbitrarily-oriented laminates, only those containing the following orientations were generated: 0°, 90°, 45°, -45°, according to typical aerospace design practices. Materials selected could be fabric-like (similar axial and transverse Young's modulus), or tape-like (significantly higher axial modulus than transverse).

3. Nondimensionalize each joint's parameters, leveraging a common approach that employs the Buckingham Pi Theorem [12]

Joints were parameterized according to the critical geometric and material properties that are of concern in the bonded joint analysis, namely:

- Adhesive and adherend thickness
- Adhesive modulus
- Overlap, free, and crack length
- Adherend ABD terms (such as A_{11} and D_{11})
- Applied axial force, bending moment, and transverse shear force

These terms were then combined into a set of nondimensionalized Pi terms via dimensional analysis. Each candidate's Pi terms were recorded along with the raw geometric and material properties that would be required to construct a FEM and execute the rapid analysis tool.

4. Reduce number of designs to a computationally tractable quantity by eliminating candidates within a threshold distance from each other in the nondimensional space

Each candidate's location was considered in the multidimensional space where each dimension corresponded to a Pi term. A desired final candidate count was prescribed to balance a large design space with limited computational resources, and candidates were iteratively removed from the "pool" of possible designs based on their proximity to each other until the desired quantity was left. Initial passes through the pool would remove only candidates which were very similar to each other, while subsequent passes would continue to remove those which exhibited slightly different traits. Typical nondimensionalized proximity (distance normalized by the maximum extent of each dimension) of points after this process was completed was 5%. This process is represented schematically for two dimensions in Fig. 4.

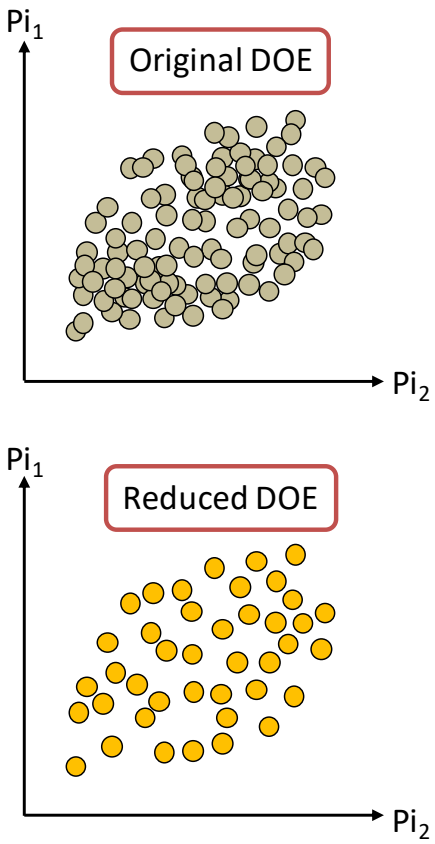

Fig. 4 Schematic Representation of Candidate Designs Before and After Thinning, Plotted in 2D Space

Once this process was completed, the final candidates were executed in both FEA and HyperSizer, and the results extracted and compared. Semi-automated inspection of the quantified difference between HyperSizer predictions and FEA results was used to determine which geometric or material values result in unacceptably large error. What constituted "unacceptably large error" is somewhat subjective, but was based on engineering judgement of the impact that parameter (or set of parameters) constraints had on the overall magnitude of error observed. These values were considered the "limits of applicability". A second round of designs were then generated only within the newly-determined limits of applicability according to the above process, and executed. These results were used to derive the final verification metrics reported in section C.

Percent difference (or error) between FEA and HyperSizer results were determined based on the predicted load factor (scaling all applied load components) that would cause an existing crack to begin to propagate, according to a simple quadratic law interacting G_I and G_{II}. This is demonstrated visually in Fig. 5, where the dotted green line represents the computed failure index according to the power law. As an example, a notional HyperSizer prediction is shown with a red dot, and the horizontal distance between this point and the green line is the difference or error.

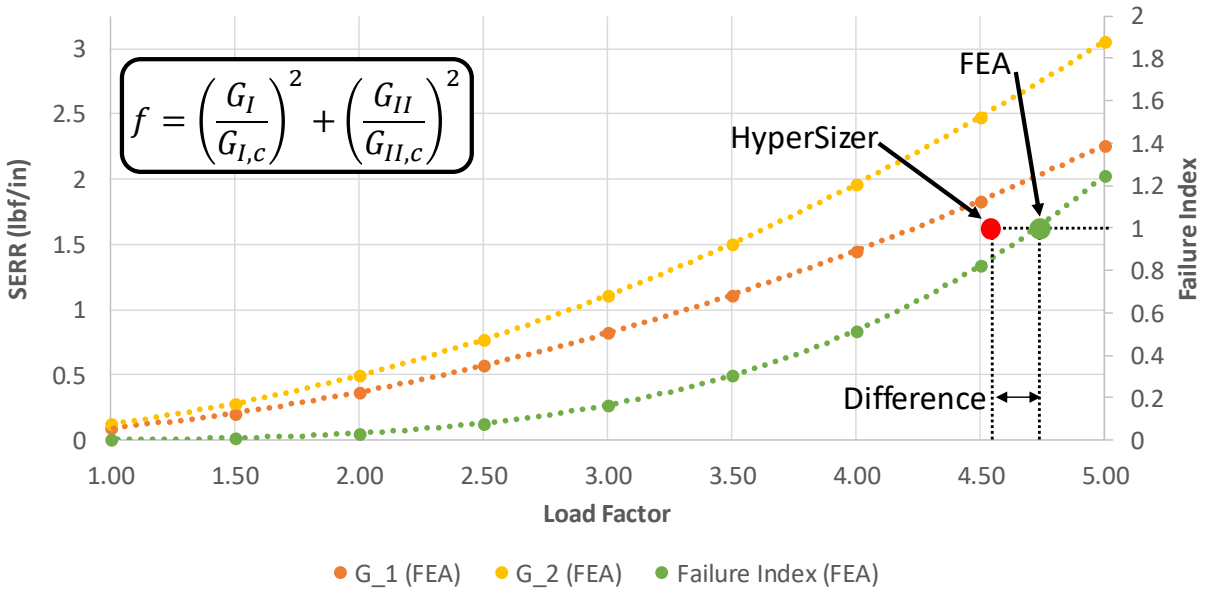

Fig. 5 Notional Comparison of HyperSizer and FEA Results for VCCT

B. Finite Element Models

As previous discussed, the intention of this verification exercise was not to confirm simply that the implementation is correct by comparing results to a mathematically identical model, as this process had already been completed previously completed [4]. Instead, this "intermediate" verification was completed to quantify the accuracy of the analysis methodology compared to a similar, known solution. For this reason, finite element models were generated to have a similar level of fidelity to that of the rapid analysis tool. Abaqus FEMs consisted of linear plane-strain elements (CPE3 and CPE4) for both the composite plies and adhesive regions, and the in-built VCCT functionality was used for computing the strain energy release rates at the crack tip. FEMs were solved using Abaqus 2018, and no geometric or material nonlinear effects were considered. Fig. 6 shows an example of a stepped lap FEM, and Fig. 7 shows a magnified view of the mesh. Early sensitivity studies were used to determine that an element length of approximately 0.01" and three elements through the thickness of each ply were sufficient to converge the computed strain energy release rates, which are typically much less sensitive to mesh density than stresses.

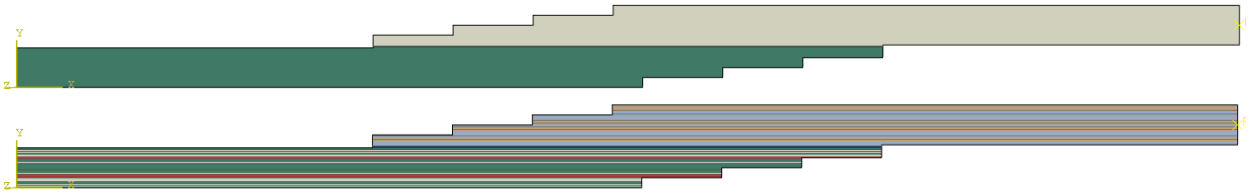

Fig. 6 An Example Single-Lap FEM Colored by Adherend (top), and by Ply Orientation (bottom).

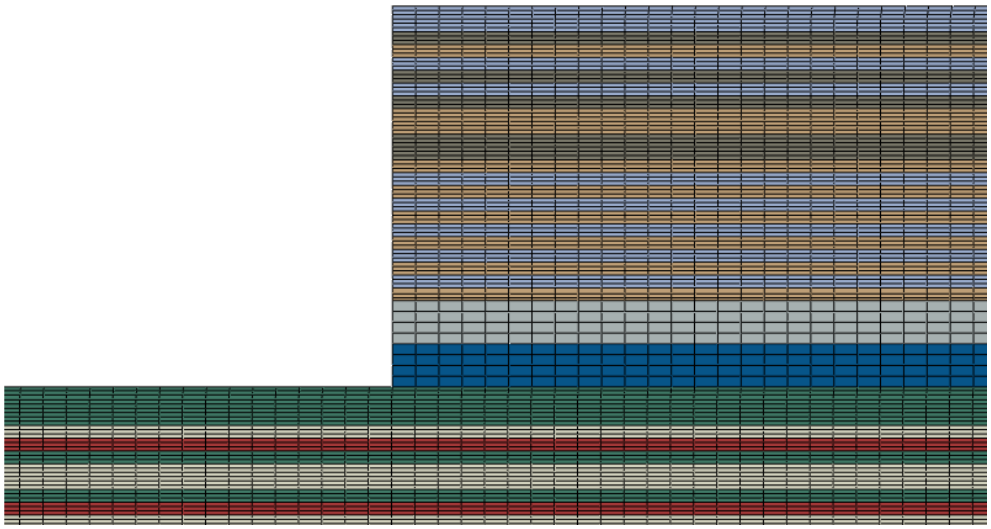

Fig. 7 Single-Lap Joint Mesh Refinement, Colored by Ply Orientation

One end of each FEM was constrained to react the loading (axial force, bending moment, transverse shear) applied to the other end. For computational efficiency, critical strain energy release rates were set arbitrarily high in the FEM to prevent the crack from actually growing. Then, strain energy release rates were extracted from the FEA results and used to compute the load factor that would cause the crack to begin to grow according to the power law described previously. Since there are no nonlinear effects contributing to the FEM behavior, the crack tip strain energy release rates scale perfectly quadratically with applied load, allowing for interpolation. This assumption was confirmed prior to beginning the verification process.

C. Verification Results

The load factor predicted by HyperSizer to cause crack growth was compared to the same quantity extracted from the finite element models, as described in section A and illustrated in Fig. 5. Approximately 2400 configurations were compared, each consisting of a unique combination of joint type (single lap, doubler, etc.), material properties, layups, and geometries (overlap lengths, adhesive thickness, etc.). The difference between HyperSizer and FEA was computed according to the below equation.

$$\%\, Difference = \left(\frac{F_{FEA} - F_{HyperSizer}}{F_{FEA}}\right) * 100 \tag{3}$$

These 2400 specimens were generated within the limits of applicability that were separately derived, as later described in section IV. The aggregated results are captured below in Fig. 8, which includes only the magnitude of difference (and not sign).

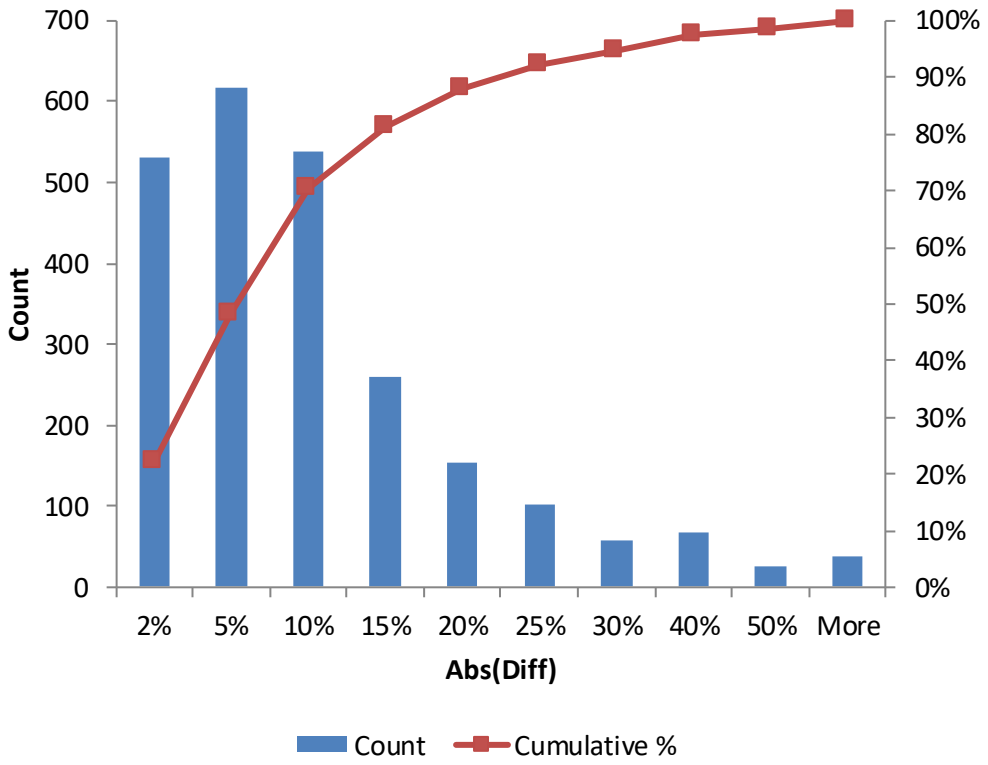

Fig. 8 Aggregated Results of Bonded Joint Verification, FEA vs. HyperSizer

The aggregated results in the histogram show difference in magnitude between HyperSizer and FEA, along with the cumulative percentage of configurations exhibiting difference of no more than each bin's label. The median difference was 5.2%, where 70% of configurations exhibited a difference of less than 10%, while 95% exhibited less than 30% difference.

When including the sign of the difference between HyperSizer and FEA, Fig. 9 shows that the difference is mostly evenly distributed between conservative (positive) and unconservative (negative). There is a slight tendency towards unconservative difference; the average difference was -2.94% and the median was -1.45% (both slightly unconservative). The standard deviation was 16.5%.

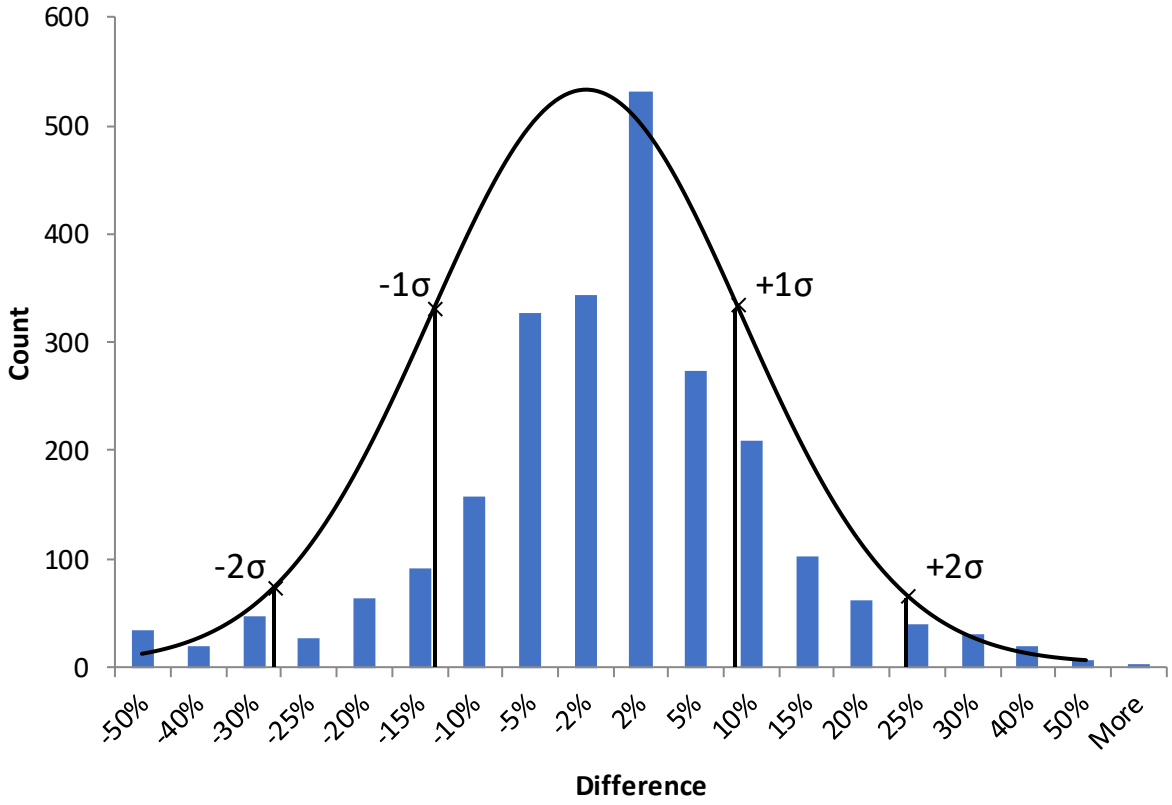

Fig. 9 Aggregated Results with Signed Error; Unconservative Difference Is Negative and Conservative Difference Is Positive. Normal Distribution Included Showing One and Two Standard Deviations. FEA vs. HyperSizer.

Overall agreement between HyperSizer and FEA was excellent. Although the FEMs were constructed to be as similar to the HyperSizer solution as feasible, fundamental differences in assumptions still remain. These differences likely explain the majority of the (still relatively small) difference between the two tools; one of the major driving differences is the treatment of the adhesive and adherends as continuums by Abaqus. In the rapid tool, the adhesive is treated as a series of uncoupled shear and tension springs, while the adherends are formulated around plate theory and classical lamination theory.

Additional differences can be explained by irregularities in the FEMs. Due to the large number being tested, generation and execution was entirely automated. The generation of the FEMs relied on Abaqus CAE's inbuilt scripting capability to create and mesh geometry. Upon inspection, a minority of FEM meshes had non-ideal features such as triangular elements on the bondline and poor transitions from coarsely-meshed to finely-meshed regions. Future investigations could incorporate tighter controls over the mesh quality or survey existing results to eliminate those which were more irregular than desired.

IV. Limits of Applicability

Limits of applicability were derived by comparing approximately 2100 configurations and manually inspecting the results to determine the bounds outside of which error became excessive. These limits are described in Table 1 below, and shown graphically in Fig. 10.

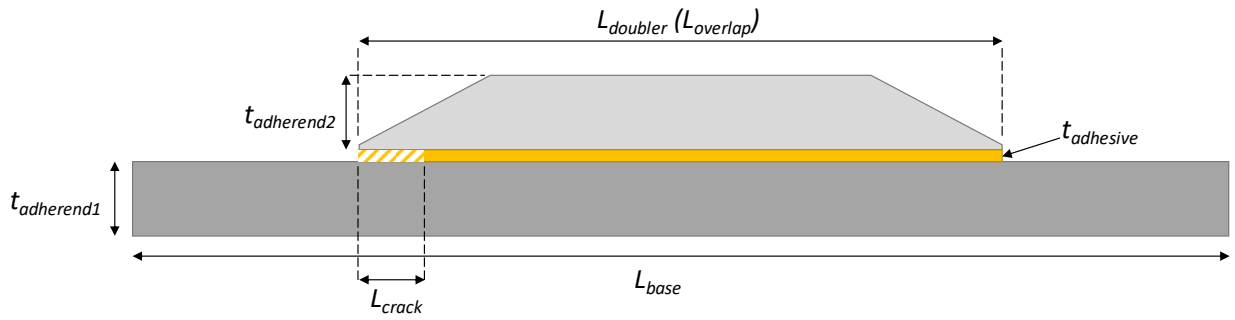

Fig. 10 Limits of Applicability Schematic

Table 1 Limits of Applicability for Bonded Joint Analysis

Variables	**Limit**	**Note**
Doubler Length, Base Laminate Length	$0.1 \leq \frac{L_{doubler}}{L_{base}} \leq 0.9$	Only applicable for doublers
Crack Length, Overlap Length	$\frac{L_{crack}}{L_{overlap}} \leq 0.75$	
Adherend 1 Thickness, Adherend 2 Thickness	$0.2 \leq \frac{t_{adherend1}}{t_{adherend2}} \leq 5.0$	
Adhesive Thickness, Adherend 1 Thickness	$\frac{t_{adhesive}}{t_{adherend1}} \leq 0.2$	
Adhesive Thickness, Adherend 2 Thickness	$\frac{t_{adhesive}}{t_{adherend2}} \leq 0.2$	
Overlap Length, Adherend 1 Thickness	$\frac{L_{overlap}}{t_{adherend1}} \geq 4.0$	
Overlap Length, Adherend 2 Thickness	$\frac{L_{overlap}}{t_{adherend2}} \geq 4.0$	

These limits of applicability were implemented into the HyperSizer stress framework. When a joint is analyzed (or selected by the sizing process as optimal) which has geometric parameters that fall outside of the limits of applicability, warnings are presented to the user in the software's process monitor as show in Fig. 11.

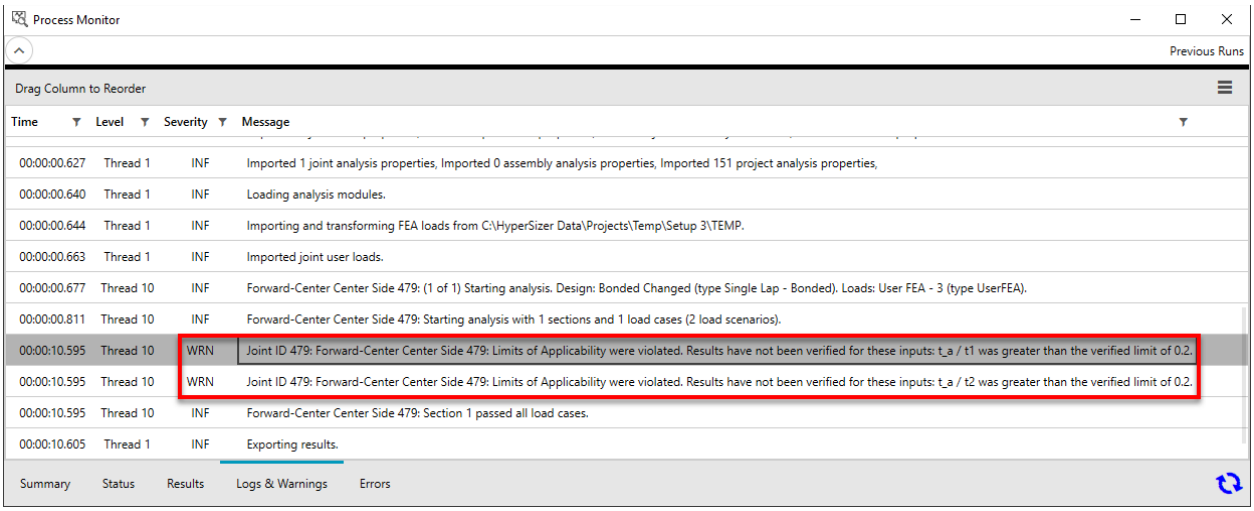

Fig. 11 HyperSizer Process Monitor Showing Two Warnings of Limits of Applicability Violations (Red Box)

Additionally, users can activate a "limits of applicability" failure criterion that will explicitly produce a negative margin of safety if an offending candidate is analyzed. The resulting negative margin is shown below in Fig. 12.

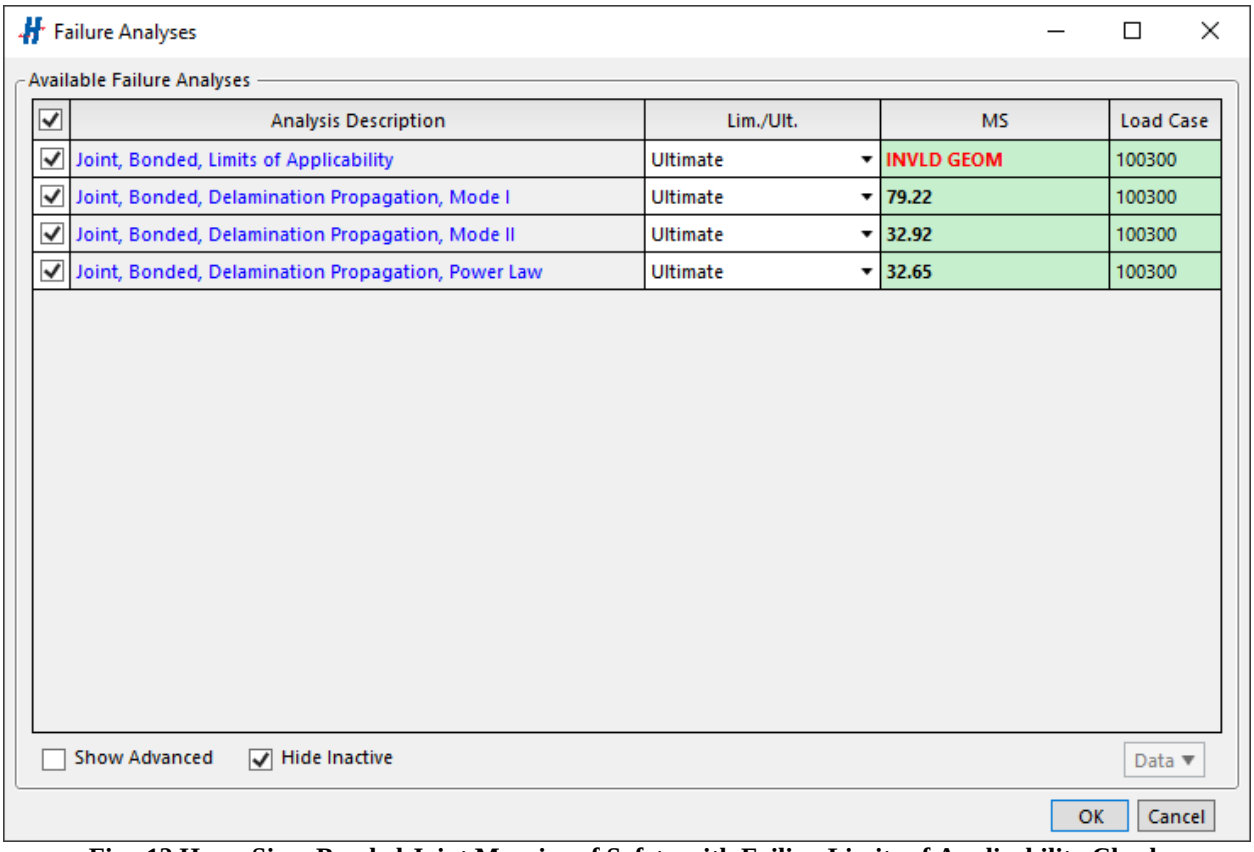

Fig. 12 HyperSizer Bonded Joint Margins of Safety with Failing Limits of Applicability Check

These two mechanisms of informing the user of potentially unverified results are intended to provide transparency and flexibility. They allow the software to size and only accept results that are within the known limits of applicability, or else freely size to the optimal design that has positive margins but still warn the user to investigate further.

V. Test Validation

A. Scope and Approach

Due to practical cost and time considerations, test validation is necessarily much more limited than FEA verification. Nevertheless, the test plan was devised in three phases in an attempt to systematically validate specimens of increasing complexity. The three phases were completed as follows:

1. **Phase 1 (Characterization)**: Test adhesive material properties to determine stress allowables, stiffnesses, and nonlinear stress-strain behavior. Other necessary quantities such as critical strain energy release rates and composite system properties had been previously determined under previous Advanced Composites Consortium (ACC) testing.
2. **Phase 2 (Calibration)**: Test simple joint configurations that have single-variable differences from a baseline. Determine if the method accurately captures the trends observed in test, and derive calibration factors if necessary.
3. **Phase 3 (Validation)**: Test more complex joint configurations, using pre-test predictions to validate that the rapid tool produces results of sufficient accuracy.

Testing focused on specimens with existing adhesive disbonds, similarly to the verification efforts described in section III. In general, error is computed with respect to the average of all test values. Some tests exhibited large scatter, so comparisons to individual test values may be misleading. In some cases, it is not possible to compare to an average due to different crack lengths being present among the specimens, and individual error calculations were performed and catalogued. The equation used to compute error with respect to FEA is shown below:

$$\%\ Error = \left(\frac{F_{Test} - F_{HyperSizer}}{F_{Test}}\right) * 100 \tag{4}$$

All test specimens were manufactured and tested at the National Institute for Aviation Research (NIAR). Manufacturing and testing were completed throughout 2018 and 2019.

B. Definition of Crack Growth

Similarly to the verification exercise documented in section III, comparisons were made between the predicted and actual load at which the embedded crack began to grow. HyperSizer predictions were made using the critical strain energy release rates of the composite material (interlaminar toughness values) rather than the adhesive, because cracks were embedded along the interface of the two, and the composite system exhibits much lower toughness. A quadratic power law was used, as shown in Fig. 5. Embedded cracks were initially grown slightly through static loading before testing to ultimate failure, to ensure a sharp crack tip exists. An image of a single lap joint being tested, showing the existence of the embedded crack, is shown below in Fig. 13.

Fig. 13 Single Lap Joint with Embedded Crack, Showing Markings Used to Track Crack Growth

When possible, the crack growth was monitored from both sides of the specimen during tests. In cases where this data was available, crack growth was defined to occur at the load that resulted in both sides exhibiting the minimum-detectable change in crack length (1mm). In cases where cracks were only monitored from one side, the load causing that side to exhibit 1mm of crack growth was used.

C. Materials and Layups

All test specimens were manufactured using the IM7/8552 tape material system. Properties used for analysis were based on those determined during previous testing under the Advanced Composites Project (ACP) [13]. Composite laminates were cured using the same cure cycle referenced in this source document. The relevant properties for HyperSizer analysis are repeated below, in Table 2.

Table 2 IM7/8552 Material Properties

Property	Value	Units
$E_{1,t}$	22.146	Msi
$E_{1,c}$	1.262	Msi
$E_{2,t}$	20.400	Msi
$E_{2,c}$	1.262	Msi
$\nu_{12,t}$	0.32	--
$\nu_{12,c}$	0.32	--
G_{12}	0.749	Msi
$G_{I,c}$	1.370	in-lb/in^2
$G_{II,c}$	4.220	in-lb/in^2
t	0.0072	in

Two unique layups were used for the test data included in this document. The stacking sequences used are described below:

Layup 1: $[45/0/-45/90]_{s2}$
Layup 2: $[45/0/-45/90/0/-45/0/45/0/\_0\_]_s$

Two adhesive materials were used, depending on the specimen: an FM 300 epoxy film adhesive and an EA 9394 paste adhesive. The properties for each of these were retrieved from public literature [14], and Poisson's ratios were assumed to be 0.3 in order to compute the Young's moduli according to Hooke's law. When part of a secondary bond (i.e. not cured simultaneously with a laminate adherend), adhesives were cured according to the cycles referenced in this source document. The material properties used for these systems are reported below in Table 3 and Table 4.

Table 3 FM 300 Material Properties

Property	Value	Units
E	0.299	Msi
G	0.115	Msi
ν	0.3	--
t	0.006	in

Table 4 EA 9394 Material Properties

Property	Value	Units
E	0.456	Msi
G	0.175	Msi
ν	0.3	--
t	0.025	in

D. Validation Results

1. Doubler Transverse 3-Point Bend

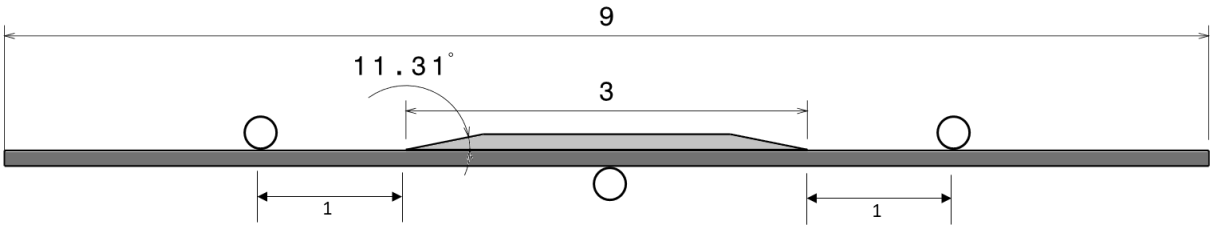

Fig. 14 Transverse 3-Point Bend Configuration. Distances are Inches.

The bonded doubler transverse 3-point bend test includes three separate predictions due to significant difference in starting crack lengths. The results are cataloged in Table 5, below. Doublers had internal ply drops to establish the taper shown in Fig. 14, and the doublers were co-bonded with film adhesive to the base laminate. Both laminates were Layup 1. Specimens measured 1.5 inches wide, with cracks inserted at the free edge.

Table 5 Doubler Transverse 3-Point Bend

Specimen	Initial Crack Length (in)	Test (lb)	HyperSizer (lb)	Error
1	0.349	200.02	186.13	6.9%
2	0.398	151.61	173.74	-14.6%
3	0.417	167.26	168.38	-0.7%
Average	**--**	**--**	**--**	**-2.8%**

2. Double Strap Joint

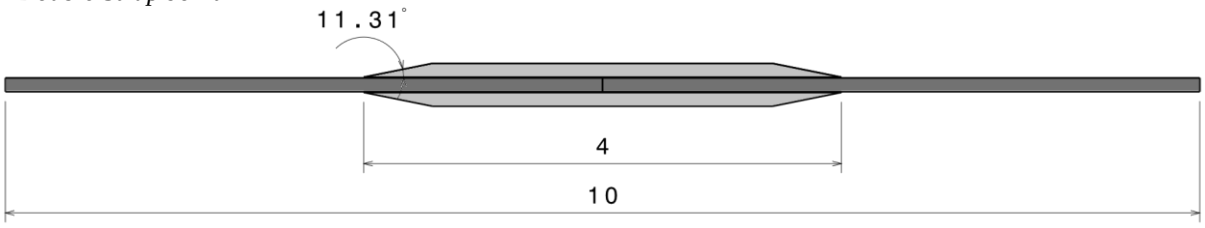

Fig. 15 Double Strap Joint Geometry. Distances are Inches.

Double strap joints were constructed via secondary bonding of the strap laminates to the base laminates using paste adhesive. Both laminates were Layup 1, and the strap taper was machined post-cure. Specimens were 1.5 inches wide, with cracks inserted at the free edge. Specimens were tested in both tension and compression. For compression tests, a small amount of contact (evidenced by compressive σ_{zz} at the crack tip) occurs, so the mode I component of strain energy release rate is neglected.

Table 6 Double Strap Tension

Specimen	Initial Crack Length (in)	Test (lb)	HyperSizer (lb)	Error
1	--	3415.12	--	--
2	--	5635.15	--	--
Average	**0.348**	**4525.13**	**5902.5**	**-30.4%**
C.V.	**--**	**24.5%**	**--**	**--**

Table 7 Double Strap Compression

Specimen	Initial Crack Length (in)	Test (lb)	HyperSizer (lb)	Error
1	--	6897.88	--	--
2	--	9228.67	--	--
3	--	5743.46	--	--
4	--	11761.28	--	--
Average	**0.467**	**8407.82**	**8337**	**0.8%**
C.V.	**--**	**27.4%**	**--**	**--**

3. Single Lap Joint, Untapered, 1.5" Overlap

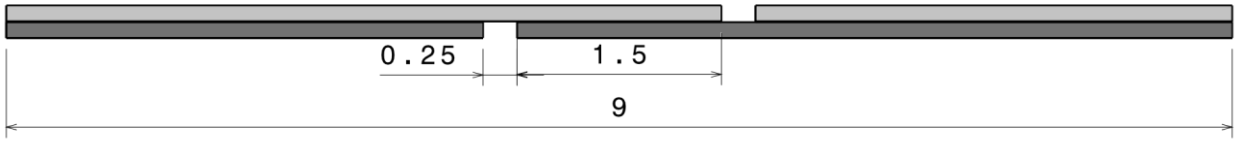

Fig. 16 Untapered 1.5" Overlap Single Lap Joint. Distances are Inches.

Single lap joints were secondarily bonded with film adhesive. Both laminates were Layup 1. Specimens were 1.5 inches wide, with cracks inserted at the free edge.

Table 8 Single Lap Joint, Untapered, 1.5" Overlap

Specimen	Initial Crack Length (in)	Test (lb)	HyperSizer (lb)	Error
1	--	2618.32	--	--
2	--	2657.71	--	--
3	--	3268.73	--	--
Average	**0.392**	**2848.25**	**2693.88**	**5.4%**
C.V.	**--**	**10.5%**	**--**	**--**

4. Single Lap Joint, Untapered, 2.0" Overlap

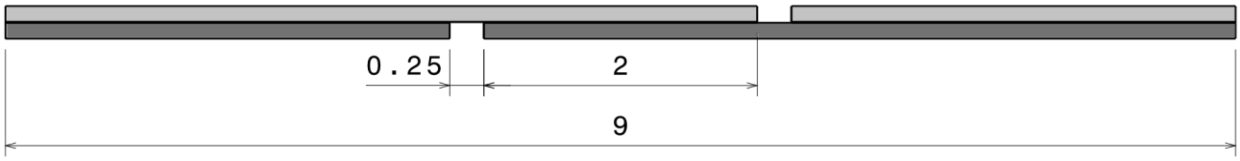

Fig. 17 Untapered 2.0" Overlap Single Lap Joint. Distances are Inches.

Single lap joints were secondarily bonded with film adhesive. Both laminates were Layup 1. Specimens were 1.5 inches wide, with cracks inserted at the free edge.

Table 9 Single Lap Joint, Untapered, 2.0” Overlap

Specimen	Initial Crack Length (in)	Test (lb)	HyperSizer (lb)	Error
1	--	3044.91	--	--
2	--	1579.01	--	--
3	--	2242.64	--	--
4	--	3445.63	--	--
5	--	1111.07	--	--
Average	**0.329**	**2284.65**	**2639.56**	**-15.5%**
C.V.	--	**38.2%**	--	--

5. Single Lap Joint, Untapered, 3.0” Overlap

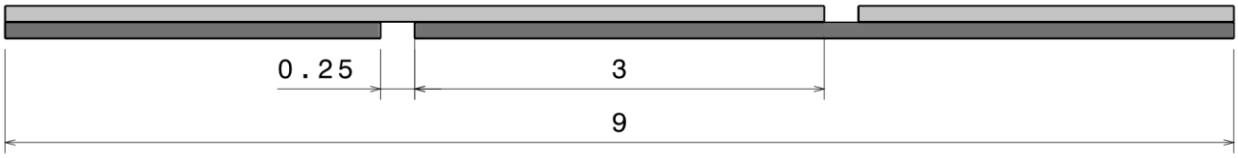

Fig. 18 Untapered 3.0" Overlap Single Lap Joint. Distances are Inches.

Single lap joints were secondarily bonded with film adhesive. Both laminates were Layup 1. Specimens were 1.5 inches wide, with cracks inserted at the free edge.

Table 10 Single Lap Joint, Untapered, 3.0” Overlap

Specimen	Initial Crack Length (in)	Test (lb)	HyperSizer (lb)	Error
1	--	3708.36	--	--
2	--	2997.22	--	--
3	--	2586.85	--	--
Average	**0.329**	**3097.47**	**2551.33**	**17.6%**
C.V.	--	**15.0%**	--	--

6. Spar Pull-Off

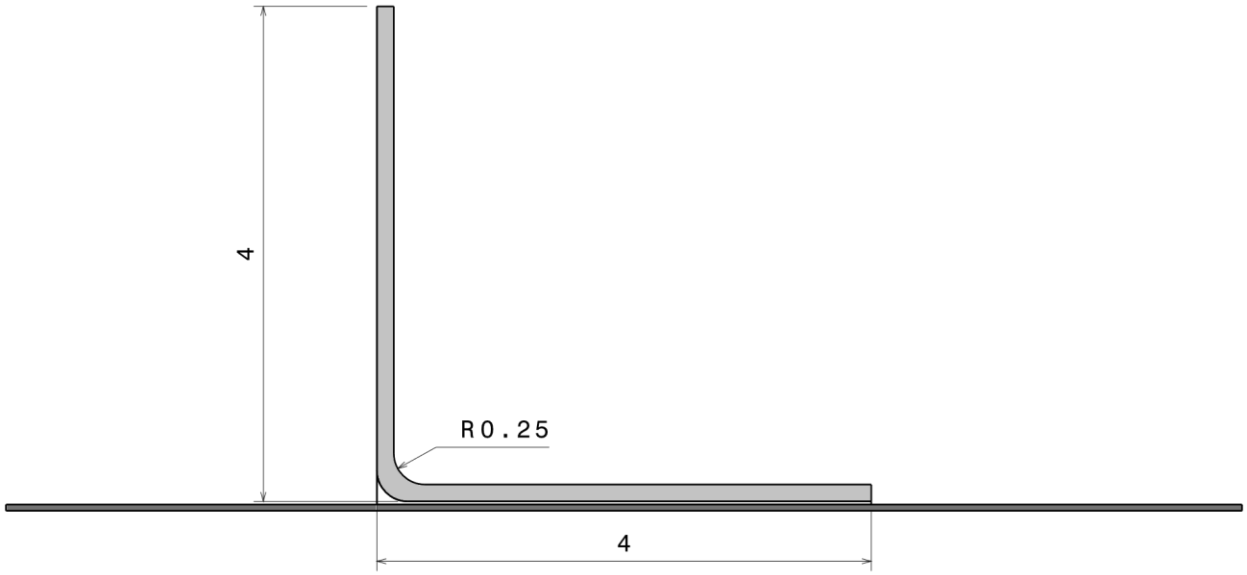

Fig. 19 Spar Pull-Off Specimen. Distances are Inches.

Spar pull-off joints were secondarily bonded with paste adhesive. Base laminate was Layup 1 and spar laminate was Layup 2. Specimens were 2 inches wide, with cracks inserted at the free edge.

Table 11 Spar Pull-Off

Specimen	Initial Crack Length (in)	Test (lb)	HyperSizer (lb)	Error
1	--	91.06	--	--
2	--	70.58	--	--
3	--	81.07	--	--
Average	**0.677**	**80.90**	**84.0**	**-3.8%**
C.V.	--	**10.3%**	--	--

VI. Implementation in the Stress Framework

HyperSizer is a software tool specializing in detailed stress sizing of stiffened panels and associated details (such as honeycomb core ramps and joints) [15]. As a stress framework, it provides a large amount of infrastructure to assist in the design and analysis of aerospace structures, such as:

- Standardized and consistent analytical analysis methods
- Material database containing allowables, stiffnesses, etc.
- Automated FEA load extraction, transformation, and processing including filtering and identification of critical conditions
- Sizing of metal and composite structure, both stiffened and unstiffened
- Global FEM management
- Iteration with FEA for load path convergence, deflection limits, and global buckling requirements
- Data exchange with external tools such as CAD packages

In HyperSizer version 8.0, considerable emphasis has been placed on the integration of analysis and sizing of joints into the overall design process. The newly-developed workflow uses the same global loads FEM for both far-field "acreage" sizing of stiffened or unstiffened panels as well as the detailed sizing and analysis of fastened and bonded joints, as illustrated in Fig. 20.

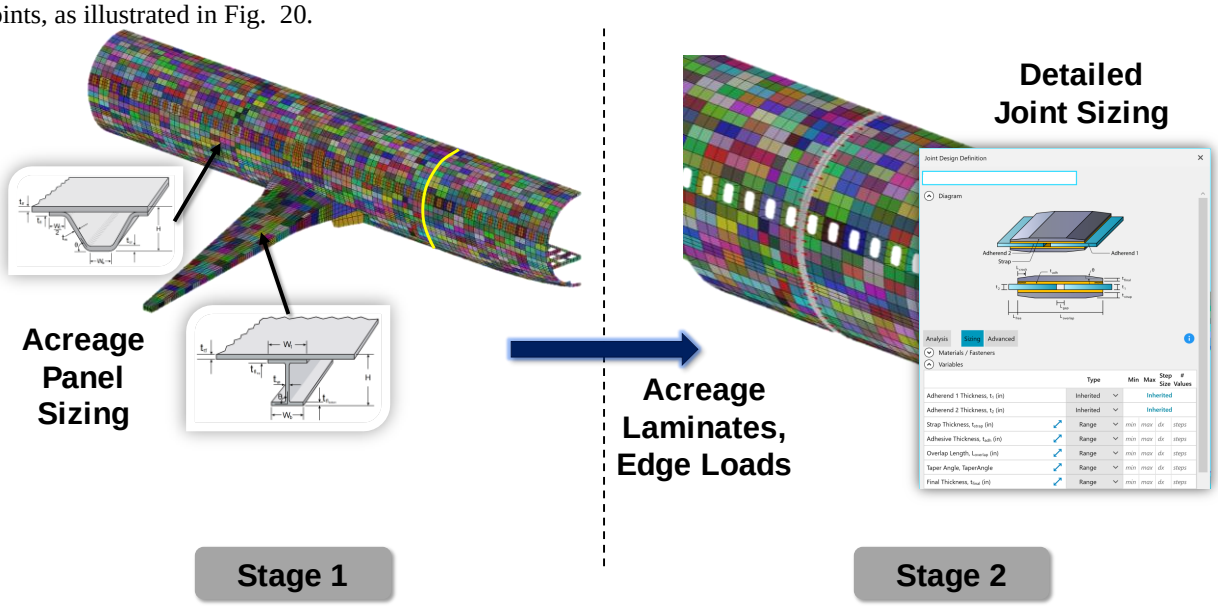

Fig. 20 Two-Stage Sizing Process, Progressing from Acreage Panel Sizing to Detailed Joint Sizing

This two-stage process allows for engineers to size acreage panels to meet strength, stiffness, and stability requirements before transitioning to more detailed sizing and analysis of the joints that may connect them. In the

second stage, the results from the far-field sizing may be "inherited" as a starting point for the joint design. If needed, these results can be overridden in the joint design, for instance to add pad-ups to account for increased local stresses due to the presence of the joint.

Joint designs are defined via software forms, allowing for user-prescribed values or sizing bounds, as shown below in Fig. 21. When sizing a joint, the software will automatically cycle through the possible candidate designs until it finds one that provides positive margins of safety for all the criteria selected by the user. The order in which candidates are evaluated may be prescribed by the user according to manufacturing preferences.

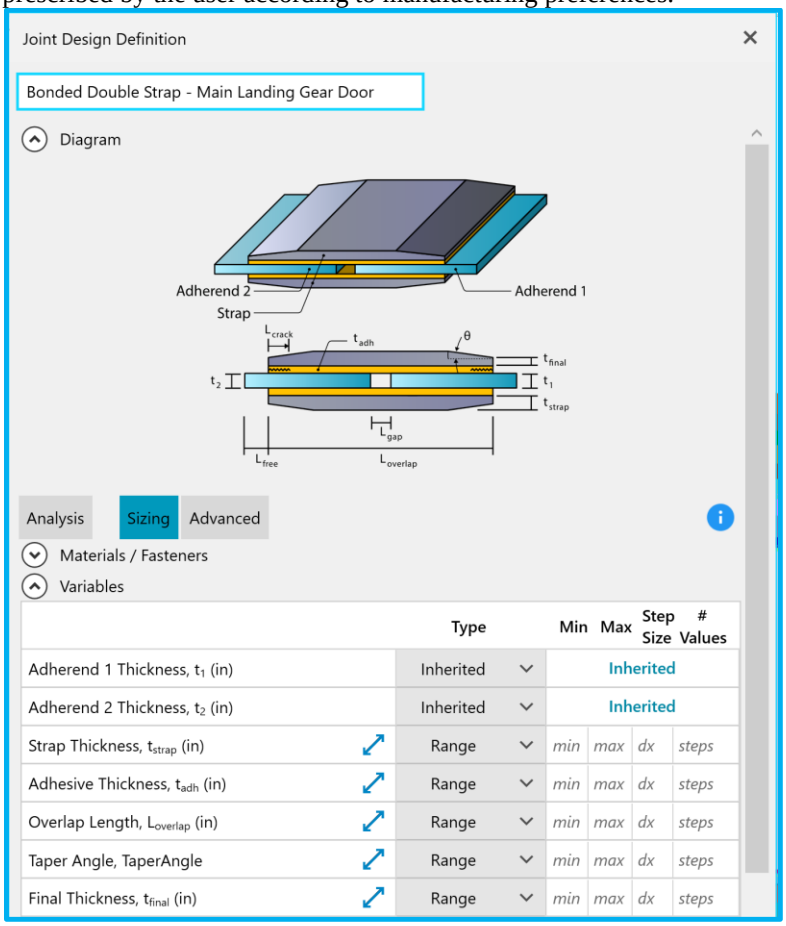

Fig. 21 Joint Design Definition, Showing Inherited Adherends and Sizing Bound Fields

Load extraction and transformation is performed automatically by the software, and the user is provided a variety of methodologies to determine design-to load conditions. These range from element-based (where the loads in each element pair for each load case are used as design-to loads), to statistical (where the loads along a joint are averaged and increased by a prescribed number of standard deviations) and peak (where metrics are used to determine which combinations of element pair and load case produce the most critical conditions). All of these selections are also made through graphical forms and applied to the model, as shown in Fig. 22.

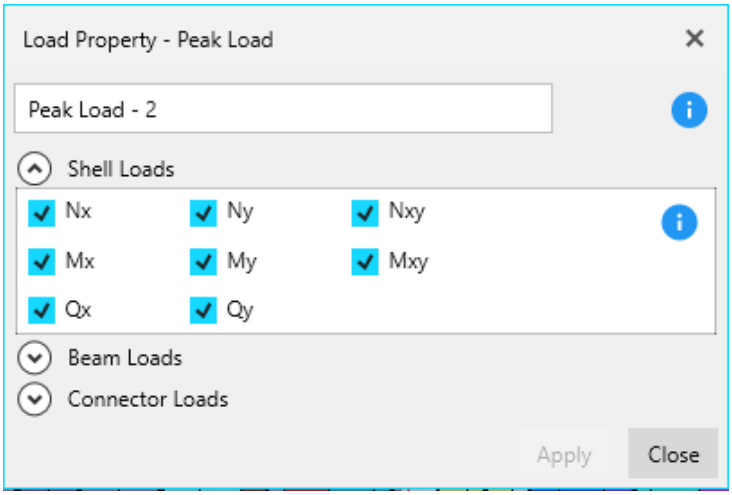

Fig. 22 Peak Load Property, Allowing User to Define Which Load Components Should Be Used for Sizing

After sizing bonded joints, results may be plotted in the graphics through an interactive legend. These data include values such as minimum margin of safety (as shown in Fig. 23), selected optimum geometry or materials, controlling load case, and critical failure criterion.

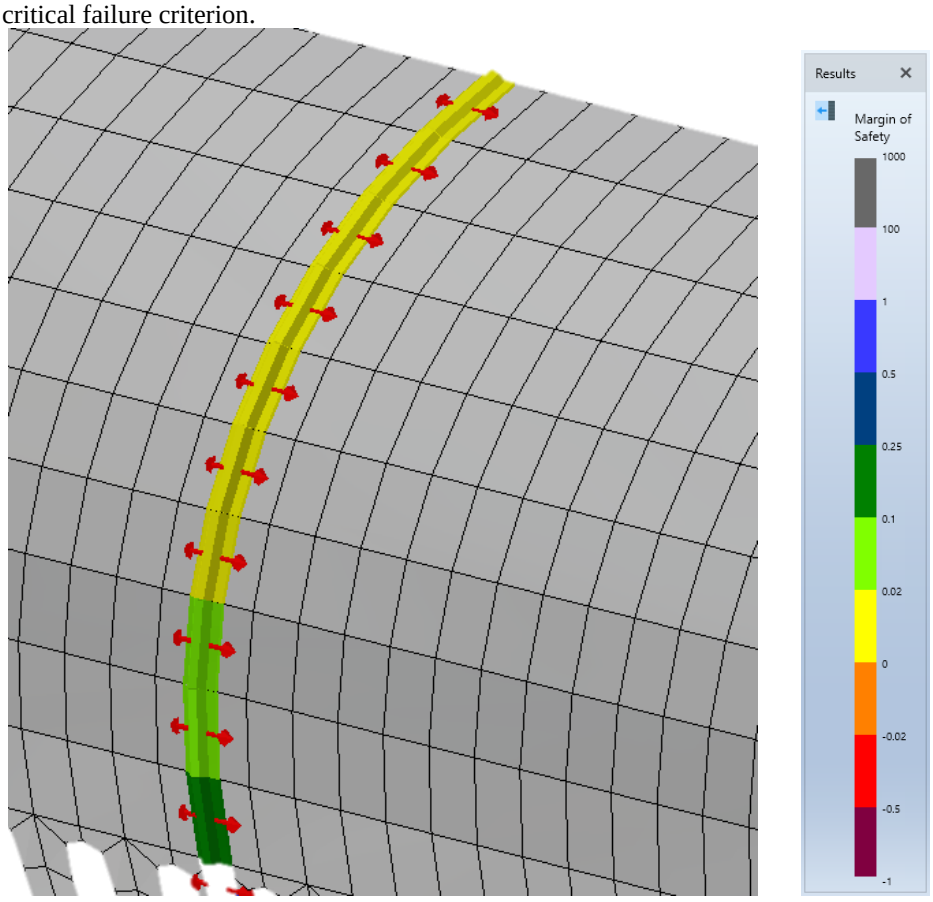

Fig. 23 Margins of Safety Plotted on Joint in Graphics Window

VII. Conclusion

The HyperSizer bonded joint rapid analysis capability was verified and validated against finite element analysis and test results for its virtual crack closure technique methodology. A verification approach was developed to ensure

rigorous coverage of the design space of interest while reducing computational overhead typically associated with broad experiments. The results of comparisons against thousands of finite element models demonstrated high accuracy; the median magnitude of difference from FEA was 5.2%, with 70% of cases under 10% difference and 95% of cases under 30% difference. Test validation was conducted with specimens manufactured and tested at the National Institute for Aviation Research in Wichita, Kansas. This validation exercise demonstrated strong agreement between HyperSizer predictions and experimental results of the applied load causing growth of an embedded crack. The magnitude of error to test ranged between approximately 1% to 30%.

The rapid analysis capability was implemented into the latest version of the HyperSizer software. In this stress framework, users can analyze and size bonded joints using the same global loads FEM that has been previously used for sizing of acreage panels. Along with enabling features such as material data management and graphical visualization of results, users are provided considerable control over the way analysis is conducted along with traceability into the process.

VIII.Acknowledgments

The material is based upon work supported by NASA under Award Nos. NNL09AA00A and 80LARC17C0004. Any opinions, findings, and conclusions or recommendations expressed in this material are those of the author(s) and do not necessarily reflect the views of the National Aeronautics and Space Administration.

References

[1] P. Yarrington, J. Zhang and C. Collier, "Failure Analysis of Adhesively Bonded Composite Joints," in *AIAA/ASME/ASCE/AHS/ASC Structures, Structural Dyanmics, and Materials Conference*, Austin, 2005.

[2] J. S. Park and J. K. Seo, "Analytical Method for Simulation of Buckling and Post-buckling Behaviour of Curved Pates," *Computer Modeling in Engineering & Sciences,* vol. 106, no. 4, pp. 291-308, 2015.

[3] F. Mortensen and O. T. Thomsen, "Analysis of Adhesive Bonded Joints: A Unified Approach," *Composites Science and Technology,* vol. 62, no. 7, pp. 1011-1031, 2002.

[4] J. Zhang, B. A. Bednarcyk, C. Collier, P. Yarrington, Y. Bansal and M.-J. Pindera, "3D Stress Analysis of Adhesively Bonded Composite Joints," in *AIAA/ASME/ASCE/AHS/ASC Structures, Structural Dynamics, and Materials Conference*, Austin, 2005.

[5] W. Ramberg and W. Osgood, "Description of Stress-Strain Curves by Three Parameters," National Advisory Committee for Aeronautics, Washington, DC, 1943.

[6] P. W. Yarrington, C. S. Collier and B. A. Bednarcyk, "Failure Analysis of Adhesively Bonded Composite Joints vai the Virtual Crack Closure Technique," in *AIAA/ASME/ASCE/AHS/ASC Structures, Structural Dynamics, and Materials Conference*, Newport, 2006.

[7] J. E. Action and S. P. Engelstad, "Crack Arrestment of Bonded Composite Joints," in *54th AIAA/ASME/ASCE/AHS/ASC Structures, Structural Dynamics, and Materials Conference*, Boston, 2013.

[8] S. Engelstad, O. Berry, G. Renieri, L. Deobald, G. Mabson, B. Dopker, E. Nottorf and S. Clay, "A High Fidelity Composite Bonded Joint Analysis Validation Study - Part I: Analysis," in *46th AIAA/ASME/ASCE/AHS/ASC Structure, Structural Dynamics & Materials Conference*, Austin, 2005.

[9] R. Krueger, "Virtual crack closure technique: History, approach, and applications," *Applied Mechanics Reviews,* vol. 57, no. 2, pp. 109-143, 2002.

[10] Collier Research Corporation, "Methods & Equations Joint Strength, Composite Bonded," 28 May 2005. [Online]. Available: http://hypersizer.com/download.php?type=analysis&file=AID160-180_Joint_Strength,_Composite_Bonded.HME.pdf.

[11] S. E. Stapleton, B. Stier, S. Jones, A. Bergan, D. W. Sleight, B. A. Bednarcyk, A. Zahn, B. Farrokh and K. N. Segal, "Comparison of Design Tools for Stress Analysis of Adhesively Bonded Joints," in *AIAA SciTech 2019 Forum*, San Diego, 2019.

[12] M. C. Albrecht, C. J. Nachtsheim, T. A. Albrecht and R. D. Cook, "Experimental Design for Engineering Dimensional Analysis," *Technometrics,* vol. 55, no. 3, pp. 257-270, 2013.

[13] S. Wanthal, J. Schaefer, B. Justusson, I. Hyder, S. Engelstad and C. Rose, "Verification and Validation Process for Progressive Damage and Failure Analysis Methods in the NASA Advanced Composites Consortium," in *American Society For Composites*, 2017.

[14] J. Tomblin, W. Seneviratne, P. Escobar and Y. Yoon-Khian, "Shear Stress-Strain Data for Structural Adhesives (DOT/FAA/AR-02/97)," Office of Aviation Research, Washington, DC, 2002.

[15] Collier Research Corporation, "HyperSizer Pro," [Online]. Available: http://hypersizer.com/pro/. [Accessed 26 11 2019].